26th International Congress of Mechanical Engineering
COBEM 2021
ABCM Associação Brasileira de Engenharia e Ciências Mecânicas
November 22-26, 2021, Virtual Congress, Brazil

COB-2021-1065
IMPACT OF THE CHORD/DIAMETER DISTRIBUTION ON PROPELLERS EFFICIENCY USING THE LIFTING-LINE THEORY

Thiago Pontin Tancredi
Felipe Leme
TEG - Thermofluids Engineering Group / LabSin - Naval Simulation Lab - Universidade Federal de Santa Catarina - Brasil
thiago.tancredi@ufsc.br
sou_feleme@hotmail.com

Abstract. *Propellers are components widely used in vessel propulsion. Paradoxically, because of the high cost associated with physical experiments and the complexity of the phenomena to be modeled, the studies of these systems remain quite restricted. To reduce this gap, this work analyzes the influence of the c/D quotient along the blade on the hydrodynamic performance of a propeller. Prandtl's Lifting-line Theory implemented in the OpenProp code is used to the analyses. Initially, it is presented a validation procedure done with experimental data available in the literature. After the validation, two groups of geometries are proposed. The first, has a constant c/D distributions and the second, has c/D values decreasing in the region close to the blade tip. This work investigated Wageningen B-Series propellers with 3, 4 and 5 blades, with EAR values between 0.45 and 0.80. The results presented allow to conclude that, for any combinations analyzed, the lower is the c/D value, the higher is the efficiency obtained, reaching increments of 9%. When propellers with lower values of c/D at the blade's tips are analyzed, the efficiencies obtained are even higher, reaching increments of 13%.*

Keywords: *propellers, lifting-line theory, c/D, propulsion, series B*

1. INTRODUCTION

Among the different subsystems present in ships, this work analyzes the propulsion one. The study will be limited to fully submerged conventional propeller. Among the various possible approaches, it is proposed to investigate the hydrodynamic efficiency, neglecting issues such as noise emission, structural strength and cavitation.

As pointed out by Watson (1998), propellers must provide a high thrust with low torque requirement. Once the performance of these systems impacts in the maximum speed and fuel consumption, studies about the optimization of propellers have great importance in ship design.

Traditionally, the propeller selection is done considering standard geometries, whose performance is known through experimental results. This approach usually occurs because the analysis of propellers is difficult since, as Molland (2008) points out, its success depends on the integration of different disciplines: hydrodynamics, acoustics, solid mechanics, metallurgy, manufacturing, among others.

Once the propeller selection requires complex numerical models with high computational cost (Molland, 2008), this work evaluates a numerical methodology based on lifting-line theory that can analyze the performance of propellers with any geometry. The numerical model used was implemented in OpenProp program and it is available in Matlab language.

This work studies the influence of the c/D quotient along the blade on a propeller hydrodynamic performance. The analysis of this parameter changed one of the most important and classic research about naval propellers. The first experimental results for propellers series were published by Lammeren (1936). But the geometries studied showed severe cavitation problems due to the small chords of the sections close the blade's tips. For this reason, intuitive changes gave rise to the famous B-Troost series, which is also known as Wageningen B-Series, published by Lammeren and Troost (1948) and Lammeren and Oosterveld (1969).

2. THEORETICAL BACKGRUND

2.1 The c/D coefficient

A propeller blade can be described as a set of foil sections positioned orthogonally to the propeller shaft (Figure 1). As seen in Carlton (2007), the sections can be displaced to twist the blade, which increases the propeller efficiency. But it is the lift of each blade section that develop thrust when the propeller is rotated.

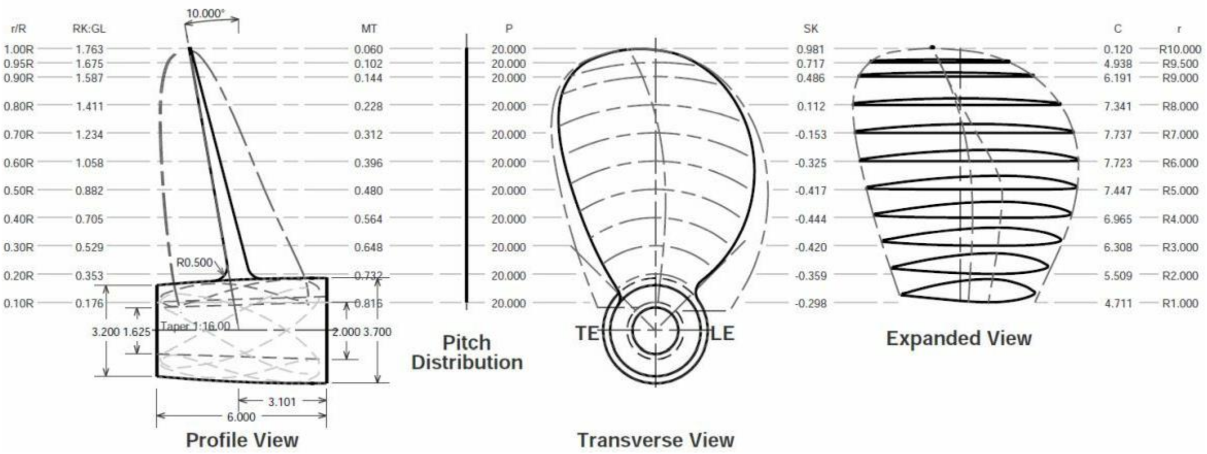

Figure 1. Foil sections along a propeller blade (MacPherson, 2020).

To define foil characteristics, this work used the standard proposed by the National Advisory Committee for Aeronautics (NACA), where the section is defined by a perpendicular cut of the blade. The chord (c) is defined as the linear length measured between the extremes of trailing edge and leading edge. In the other hand, the thickness (t) is defined as the maximum perpendicular distance between the suction side and the pressure side (Figure 2).

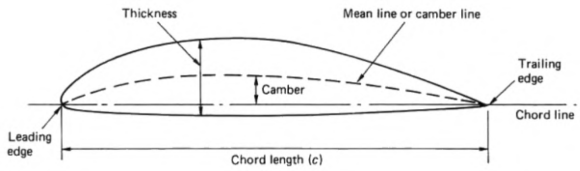

Figure 2. General definition of a foil section (Carlton, 2007).

Usually, each blade section has different values of thickness and chord. So, it is possible to define *c/D* and *t/D* quotients for each blade section, where the D is the propeller diameter.

2.2 The lifting-line theory

Anderson (2001) presents an approach for lift evaluation that uses the Kutta-Joukowski theorem to analyze the characteristics of the flow around the blade: velocity field, Γ circulation, density and free current velocity. In this approach, Equation 1 calculate the lift per wingspan of a folio subjected to uniform flow.

$$L' = \rho_\infty * V_\infty * \Gamma, \tag{1}$$

In this case, the geometry is modeled as an infinite span folio subjected to flow with a free current velocity $V_\infty$and an angle of attack α in relation to the chord line of the profile. Given these characteristics, the phenomenon is governed by Kelvin's theorem and Kutta's conditions (ANDERSON, 2001).

The same concepts used in folios analysis can be expanded for wings analysis, and, ultimately, to propellers analysis. In this case, the analyzed geometry corresponds to a set of sections along to a finite span, which defines a three-dimensional body subject to a three-dimensional flow (MISES, 1965).

The flow along a wing tends to follow towards the tips of the blade due to the pressure gradient existing between the lower surface (high pressure) and the upper surface (low pressure). Due to this behavior, vortices are generated close to the blade tip, which are responsible for the induced velocity component called downwash, which one has a downward vertical direction (ANDERSON, 2001).

The downwash induces a lift vector $\vec{L}$ perpendicular to the relative velocity vector. Once the formation of vortices is understood, it is possible to quantify the induced velocities caused by this phenomenon. Anderson (2001) presents a formulation to induced velocity $\vec{V_\iota}$ which uses the Biot-Savart law (Equation 2). In this case, the flow circulation Γ causes the induced velocity increment $d\vec{V_\iota}$ considering a portion $d\vec{l}$ of a vortex filament distant $\vec{r}$ from point P.

$$d\vec{V_\iota} = \frac{\Gamma}{4*\pi} * \frac{d\vec{l} \times \vec{r}}{|\vec{r}|^3}, \tag{2}$$

If the filament extends from minus infinity to infinity, an integration at these limits will result in the total induced velocity $\vec{V_i}$ in point P caused by the vortex.

Still about vortices, Anderson (2001) presents Helmholtz's theorem applied to incompressible and inviscid flows, which can be summarized in two postulates. The first refers to the force magnitude of a vortex filament, that must be constant along the length of the filament. The second says that a vortex filament cannot end inside a fluid, and it must extend to the limits of the fluid or forms a closed path inside the flow.

According to Abbott and Doenhoff (1959), the lifting-line theory was developed by Prandtl and colleagues during the 1910s, using Helmholtz's theorem. His study was about a linear vortex filament located under a finite wing (wingspan b) which is connected to wing tip vortices (escape vortices). Such configuration, containing a fixed vortex on the wing in combination with the vortexes at the tips, is called horseshoe vortex (Figure 3). To avoid the divergence of velocity field close of the wing extremes, Prandtl proposed a model with infinite horseshoe vortices arranged linearly under the wing, thus originating the so-called lifting line.

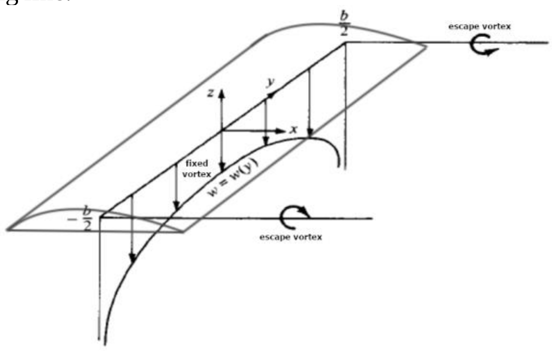

Figure 3. Horseshoe vortex with coordinate system (Anderson, 2001).

As seen in Equation 2, any segment of the vortex (*dx)* will induce a velocity at y_0 with magnitude and direction given by the Biot-Savart law. Consequently, the total induced velocity is obtained by integrating the induced velocity along the vortex sheet, that is, along the entire lifting line (Equation 3).

$$w(y_0) = -\frac{1}{4*\pi}\int_{-b/2}^{b/2}\frac{(d\Gamma/dy)\,dy}{y_0 - y}, \tag{3}$$

Once the induced velocity at a point of the lifting line is determined, other variables can be calculated, resulting in the main equation of the lifting line theory:

$$\propto (y_0) = \frac{\Gamma(y_0)}{\pi*V_\infty*c(y_0)} + \propto_{L=0} + \frac{1}{4*\pi}\int_{-b/2}^{b/2}\frac{(d\Gamma/dy)\,dy}{y_0 - y}, \tag{4}$$

Mises (1959) highlights the importance of the Equation (4), which has only one unknown variable, the circulation $\Gamma(y_0)$. Thus, the solution of the model will require the determination of this variable, which is the focus of aerodynamic studies. Finally, other important equations arise from the solution of the Equation 4, such as the total lifting L (Equation 5) and the total induced drag D_i (Equation 6).

$$L = \rho_\infty * V_\infty * \int_{-b/2}^{b/2}\Gamma(y_0)\,dy \tag{5}$$

$$D_i = \rho_\infty * V_\infty * \int_{-b/2}^{b/2}\Gamma(y_0) * \alpha_i(y_0)dy \tag{6}$$

3. METHODOLOGY

First, the validation of the technique/tool will be presented, which will be based on a propeller of Wageningen B-Series, whose characteristics (geometric and performance) are documented in the literature. After the validation phase, the parametric study will analyze a set of geometries whose characteristics are systematically varied to quantify the influence of c/D quotient along the blade on the propeller performance.

As cited before, the tool used is an open code developed by MIT researchers for the Matlab environment, and it is available on the developers' page (DARTMOUTH ENGINEERING, 2014). The OpenProp code requires the propeller geometry to evaluate the hydrodynamic performance using the lifting-line theory. After the analysis, the program plots the open water diagrams of propeller.

According to Epps (2016), the lifting-line theory is appropriate for the analysis of propellers used in vehicles and turbines. Although the theory considers an inviscid fluid, the inclusion of the C_d coefficient of each blade section allows the code to include the viscosity effects in calculate.

To validate the methodology used, the OpenProp's results for the Wageningen B4-85 propeller (four blades and EAR equal to 0.85) are compared with the experimental data from Kuiper (1992). The characteristics of B4-85 propeller are shown in Table 1.

Table 1. Propeller's data used in validation process

Parameters	**Symbol**	**Value**
Diameter [m]	D	0.25
Number of blades	Z	4
Expanded area ratio	EAR	0.85
Rotation [rps]	N	15
Pitch/Diameter ratio	P/D	0.5 to 1.4
Specific mass (salt water) [kg/m³]	ρ	1.025
Advance coefficient	J	0 to 1.15

Since the technique used by OpenProp requires the data integration along the blade, the calculated value will depend on the discretization used in the process (Epps and Kimball, 2013). So, a mesh convergence study is presented together with validation process.

Once the methodology was validated, a parametric study with different blade numbers and EAR ratios is presented. The combinations of between blades number and EAR ratios were selected to cover the range of propellers commonly used in medium and large ships.

4. DEVELOPMENT

4.1 Mesh convergence study

To apply the lifting-line theory, the program divides the blade geometry into two directions (Table 2). The first discretization occurs radially along the blade (radial panels), while the second discretization occurs along the chord line (chord panels).

Although, as discussed by Epps and Kimball (2013), the discretization in chord direction is necessary only for the three-dimensional lifting theory, the discretization suggested by the program consists of 20 radial panels and 20 chord panels. Thus, the mesh convergence study was done using the propeller whose dimensions are shown in Table 1 and considered the discretization values of 3, 5, 10, 15, 20, 25 and 30 panels in each direction.

The results using each mesh studied was compared with experimental data provide by Kuiper (1992). The mean error calculated (Table 2) considers the mean between the errors of each advance coefficient (*J*) evaluated in each *P/D* analyzed.

Table 2. Mean errors from the different meshes used.

Parameter	**Symbol**	**Radial Panels**	**Chord Panels**		
			20	**15**	**5**
Thrust coefficient	K_T	30	5.62%	*	5.64%
Torque coefficient	K_Q	30	2.01%	*	2.01%
Efficiency	η	30	20.69%	*	20.72%
Thrust coefficient	K_T	20	10.23%	10.23%	*
Torque coefficient	K_Q	20	2.79%	2.79%	*
Efficiency	η	20	20.48%	20.48%	*
Thrust coefficient	K_T	5	12.09%	*	*
Torque coefficient	K_Q	5	3.00%	*	*
Efficiency	η	5	17.74%	*	*
Thrust coefficient	K_T	3	*	*	13.89%
Torque coefficient	K_Q	3	*	*	3.19%
Efficiency	η	3	*	*	16.22%

* Combination not evaluated.

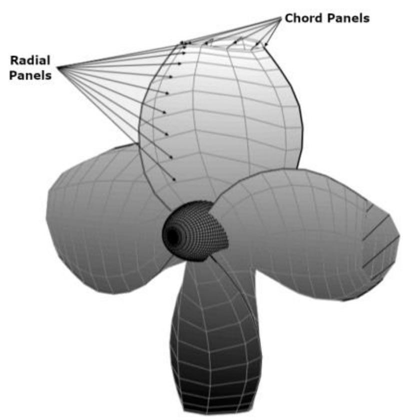

From the results seen in Table 2, it is possible to verify that discretization of the chord direction has little influence on the precision of analyses. On the other hand, the results are sensitive to the discretization in the radial direction of the blades.

Furthermore, it is interesting to mention that the convergence time, even in cases where discretization reached 50 panels in each direction, does not exceed 40 seconds, allowing the use of high discretization values. For comparison purposes, a simulation using a discretization of 10 panels in each direction takes around 18 seconds.

Finally, considering the time consumed and the quality of solution, it was decided to use a mesh with 20 radial panels and 30 chord panels. Like most simulation techniques, the lifting-line theory allows the analysis of full-size thrusters or reduced-scale models. Evidently, the appropriated discretization will change with the model size, but the differences between the approaches is beyond the scope of this work and remains as recommendation for future works.

4.2 Validation of the technique/tool used

The validation process used the Wageningen B4-85 propeller, whose geometric characteristics and the open water diagrams are shown in Kuiper (1992). To evaluate the propeller hydrodynamic performance, the OpenProp requires the description of the blade geometry. First, the chord length must be calculated for each section along the radius using Equation 7. Once the diameter (*D*), the EAR ratio and number of blades (*Z*) are fixes, the constant K(r) determines the blade's contour.

$$c(r) = \frac{K(r) * D * EAR}{Z} \tag{7}$$

The second parameter of the blade geometry description is the ratio between section thickness and propeller diameter (*t/D*), which must be defined for each section along the radius. These values are also described in Kuiper (1992) and are not discussed in this work.

Finally, the *skew* (Equation 8) and *rake* (Equation 9) are calculated from the values proposed for the *skew/c* and *rake/D* coefficients defined for each section along the blade. It is important to note that, according to Kuiper (1992), all propellers of Wageningen B-Series have a constant rake angle (θ_{rake}) of 15º.

$$\theta_{skew} = arctan\left(\frac{skew}{\left(\frac{r}{R}\right)*D*0.5}\right) \tag{8}$$

$$rake = \left(\frac{r}{R}\right) * \tan(\theta_{rake}) * 0.5 * D \tag{9}$$

Table 3 summarizes the values used in the analysis of the Wageningen B4-85 propeller, which is modeled using the geometry described by Kuiper (1992).

Table 3. Description of the Wageningen B4-85 propeller with 0.25 m of diameter

r/R	**K(r)**	***skew*/c(r)**	**c(r) [m]**	***skew* [m]**	***c*/D**	**t/D**	$\boldsymbol{\theta_{skew}}$**[°]**	***rake* [m]**	***rake*/D***
0.2	1.662	0.117	0.088	0.010	0.353	0.0366	22.45	0.007	0.027
0.3	1.882	0.113	0.100	0.011	0.400	0.0324	16.77	0.010	0.040
0.4	2.050	0.101	0.109	0.011	0.436	0.0282	12.41	0.013	0.054
0.5	2.152	0.086	0.114	0.010	0.457	0.0240	8.94	0.017	0.067
0.6	2.187	0.061	0.116	0.007	0.465	0.0198	5.40	0.020	0.080
0.7	2.144	0.024	0.114	0.003	0.456	0.0156	1.79	0.023	0.094
0.8	1.970	-0.037	0.105	-0.004	0.419	0.0114	-2.22	0.027	0.107
0.9	1.582	-0.149	0.084	-0.013	0.336	0.0072	-6.35	0.030	0.121
1.0	-	-	-	-	-	0.0030	-11.95 **	0.033	0.134

* Until version v3.3.4 do OpenProp, the interface shows just *rake*, but the code requires *rake/D*.

** Extrapolated using the cubic trendline created with the values between 0.2R and 0.9R.

It is important to note that the sections of a Wageningen B-Series propeller have a specific profile geometry. However, as pointed out by Kuiper (1992), the open water diagrams can be used for propellers with different sections profile, since the lift for the attack angle equal to zero be corrected.

Unfortunately, there is no way to correct the inclination angles of the sections manually in OpenProp. Nonetheless, the use of parameters *c/D* and *t/D* for modeling the sections assure the necessary similarity with the sections described in the Wageningen B-Series.

Finally, to mitigate problems of numerical convergence, it is important to use a value of *c/D* equal to 0.001 at the section located at r/R equal to 1. Besides, the default value of 0.008 was used to the drag coefficient (C_d) in all sections along the blade.

The performance results of Wageningen B4-85 propeller at operating point J equal to 1 are summarized in Table 4, where is shown a small difference between the OpenProp results and the experimental data of Kuiper (1992).

Table 4. Comparison of the numerical analysis (OpenProp) and experimental data of Wageningen B4-85 propeller

Parameter	Symbol	Experimental (Kuiper, 1992)	OpenProp	Error %
Advance coefficient	J	1.000	1.000	0.600
Thrust coefficient	K_T	0.127	0.123	0.001
Torque coefficient	K_Q	0.028	0.027	0.086
Efficiency	η	0.700	0.718	1.125
Thrust [N]	T	111.62	110.88	0.000
Pitch/Diameter ratio	P/D	1.200	1.158	4.200
Expanded area ratio	EAR	0.85	0.80	5.000
Advance velocity [m/s]	V_a	3.75	3.77	0.000

The differences observed in Table 4 can be understood observing that the EAR and *P/D* values calculated by the OpenProp were different from the analysis input values. Since there are no alternatives that improve the modeling algorithm used in OpenProp, an iterative procedure was done. The modelling procedure was feeding back until the modeled geometry match with design parameters.

Following the iterative procedure, Figure 4 presents a comparison between the numerical results obtained in OpenProp with the results described by Kuiper (1992).

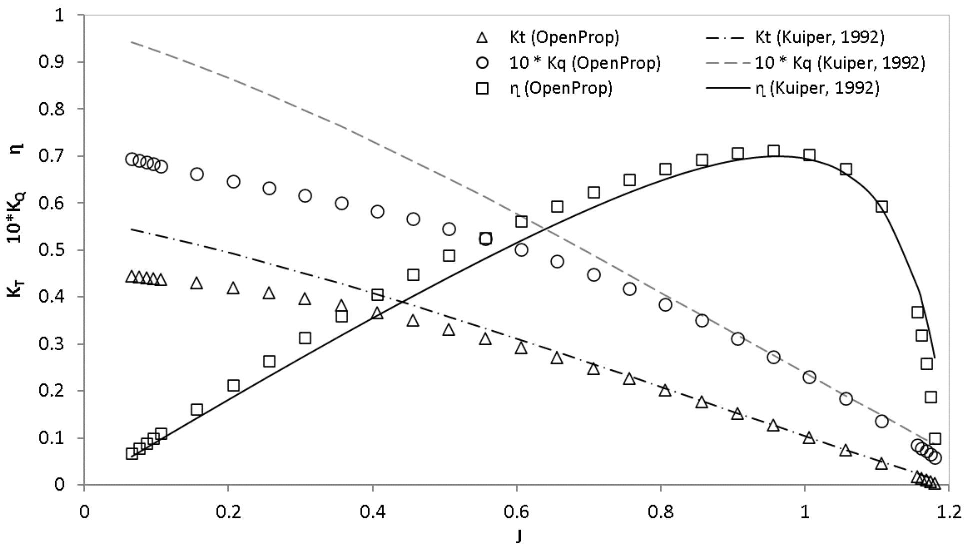

Figure 4. Comparison of the numerical analysis (OpenProp) and experimental data of Wageningen B4-85 propeller

How can be seen in Figure 4, the results obtained via OpenProp presented significant deviations from the experimental data when advance coefficient is lower than 0.3 or higher than 1.1. The statistical summary of the relative errors considering only advance coefficient *J* between 0.3 and 1.1 is shown in Table 5.

Table 5. Error between the numerical analysis (OpenProp) and experimental data of Wageningen B4-85 propeller

Parameter	Symbol	Mean Error	Standard deviation*	Maximum Error
Thrust coefficient	K_T	4.88%	3.97%	12.09%
Torque coefficient	K_Q	10.26%	7.28%	22.67%
Efficiency	η	6.38%	4.59%	13.68%

* Sampled standard deviation (*0.3 < J < 1.1)*

The statistical summary (Table 5) allows to conclude that the developed procedure presents results consistent with the literature, especially if it was considered that the lifting-line theory is a 2D approach that negligence the 3D aspects of flow.

5. PARAMETRIC ANALYSIS

In this section are presented the parametric analysis used to quantify the influence of the distribution of c/D along the blade on hydrodynamic performance of a propeller. All analyzes in this section considered the specific mass of the fluid of 1025 kg/m³, a diameter of 6 m and used the discretization of 20 radial panels and 30 chord panels.

The analyzed parameters combinations considered the most used configurations in merchant ships and focused on the cases with experimental data without interpolation. It was analyzed three blades' numbers (*Z*) and three EAR, that totalize 9 initial geometries (Figure 5).

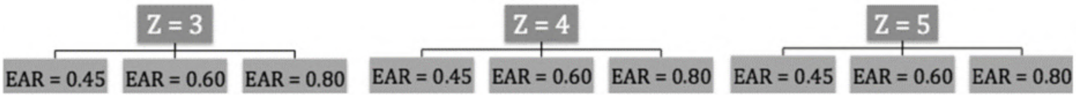

Figure 5. Combinations used in parametric analysis

Each combination of Figure 5 was modified 20 times with different values of *c*/D quotients along of the blade, that resulted in 189 geometries analyzed. In this work, only the results of three geometries are presented: B3-45, B4-80 and B5-60. There is nothing special about these three geometries, but they represent a good variability of design space.

The geometries were modelled using the procedure described in Kuiper (1992). The blade geometries characteristics of the propellers B3-45, B4-80 and B5-60 are shown in Table 6 and are the exact parameters used in OpenProp to evaluate the hydrodynamic performance of each geometry.

Table 6. Description of the analyzed geometries

Common to all			B3-45 (Z = 3 and EAR = 0.45)				B4-80 (Z = 4 and EAR = 0.80)				B5-60 (Z = 5 and EAR = 0.60)			
r/R	K(r)	*skew*/c(r)	c/D	θ_{skew}*1	t/D	*rake*/D*2	c/D	θ_{skew}*1	t/D	*rake*/D*2	c/D	θ_{skew}*1	t/D	*rake*/D*2
0.2	1.662	0.117	0.249	16.26	0.0406	0.027	0,332	21,25	0.0366	0.027	0.199	13.13	0.0326	0.027
0.3	1.882	0.113	0.282	12.01	0.0359	0.040	0,376	15,83	0.0324	0.040	0.226	9.66	0.0289	0.040
0.4	2.050	0.101	0.308	8.83	0.0312	0.054	0,410	11,70	0.0282	0.054	0.246	7.08	0.0252	0.054
0.5	2.152	0.086	0.323	6.34	0.0265	0.067	0,430	8,42	0.0240	0.067	0.258	5.08	0.0215	0.067
0.6	2.187	0.061	0.328	3.82	0.0218	0.080	0,437	5,08	0.0198	0.080	0.262	3.05	0.0178	0.080
0.7	2.144	0.024	0.322	1.26	0.0171	0.094	0,429	1,68	0.0156	0.094	0.257	1.01	0.0141	0.094
0.8	1.970	-0.037	0.296	-1.57	0.0124	0.107	0,394	-2,09	0.0114	0.107	0.236	-1.25	0.0104	0.107
0.9	1.582	-0.149	0.237	-4.49	0.0077	0.121	0,316	-5,98	0.0072	0.121	0.190	-3.60	0.0067	0.121
1.0	-	-	0.001	-8.52*	0.0030	0.134	0,001	-11,27*	0.0030	0.134	0.001	-6.85*	0.0030	0.134

* Extrapolated using the cubic trendline created with the values between 0.2R and 0.9R.
*1 Until version v3.3.4 do OpenProp, the interface shows just *skew*, but the code requires $\boldsymbol{\theta_{skew}}$.
*2 Until version v3.3.4 do OpenProp, the interface shows just *rake*, but the code requires *rake/D*.

The study was separated into two groups. In the first, each geometric variation has a different value of c/D that is constant along the blade radius (Figure 6a). But in the second group, the c/D values decrease linearly after the half of blade radius (Figure 6b). As can be seen in Figure 6a, eventually, the 3D representation of the propeller can cause the illusion that the *c/D* is not constant.

a)

b)

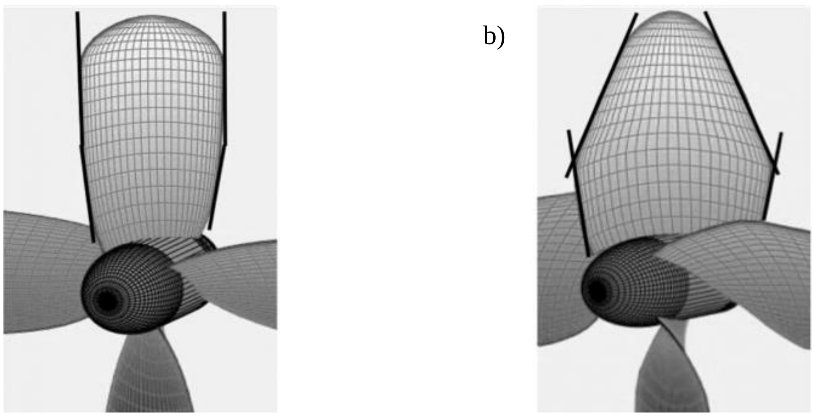

Figure 6. Typical geometry of group 1 (left) and group 2 (right)

The parametric variations of the B3-45 propeller can be seen in Table 7, while the variations of B4-80 propeller can be seen in Table 8. Finally, the variations of B5-60 propeller are shown in Table 9. To exemplify the variations analyzed, in Annex 1 are shown pictures of each one of the 20 variations done from the B4-80 propeller.

Table 7. Parametric variation of *c*/D (B3-45 propeller)

B3-45	**r/R**	**0.2**	**0.3**	**0.4**	**0.5**	**0.6**	**0.7**	**0.8**	**0.9**	**1.0**
	Original	0.2493	0.2823	0.3075	0.3228	0.3281	0.3126	0.2955	0.2373	0.0010
Group 1. c/D constant along the blade	Alteration 1	0.1800	0.1800	0.1800	0.1800	0.1800	0.1800	0.1800	0.1500	0.0010
	Alteration 2	0.2000	0.2000	0.2000	0.2000	0.2000	0.2000	0.2000	0.1700	0.0010
	Alteration 3	0.2200	0.2200	0.2200	0.2200	0.2200	0.2200	0.2200	0.1900	0.0010
	Alteration 4	0.2400	0.2400	0.2400	0.2400	0.2400	0.2400	0.2400	0.2100	0.0010
	Alteration 5	0.2600	0.2600	0.2600	0.2600	0.2600	0.2600	0.2600	0.2300	0.0010
	Alteration 6	0.2800	0.2800	0.2800	0.2800	0.2800	0.2800	0.2800	0.2500	0.0010
	Alteration 7	0.3000	0.3000	0.3000	0.3000	0.3000	0.3000	0.3000	0.2700	0.0010
	Alteration 8	0.3200	0.3200	0.3200	0.3200	0.3200	0.3200	0.3200	0.2900	0.0010
	Alteration 9	0.3400	0.3400	0.3400	0.3400	0.3400	0.3400	0.3400	0.3100	0.0010
	Alteration 10	0.3600	0.3600	0.3600	0.3600	0.3600	0.3600	0.3600	0.3300	0.0010
Group 2. c/D decreases close to tip	Alteration 1	0.1800	0.1800	0.1800	0.1800	0.1500	0.1200	0.0900	0.0600	0.0010
	Alteration 2	0.2000	0.2000	0.2000	0.2000	0.1700	0.1400	0.1100	0.0800	0.0010
	Alteration 3	0.2200	0.2200	0.2200	0.2200	0.1900	0.1600	0.1300	0.0950	0.0010
	Alteration 4	0.2400	0.2400	0.2400	0.2400	0.2100	0.1700	0.1300	0.0950	0.0010
	Alteration 5	0.2600	0.2600	0.2600	0.2600	0.2200	0.1800	0.1400	0.1000	0.0010
	Alteration 6	0.2800	0.2800	0.2800	0.2800	0.2400	0.2000	0.1600	0.1100	0.0010
	Alteration 7	0.3000	0.3000	0.3000	0.3000	0.2600	0.2200	0.1700	0.1150	0.0010
	Alteration 8	0.3200	0.3200	0.3200	0.3200	0.2800	0.2300	0.1800	0.1300	0.0010
	Alteration 9	0.3400	0.3400	0.3400	0.3400	0.3000	0.2500	0.2000	0.1400	0.0010
	Alteration 10	0.3600	0.3600	0.3600	0.3600	0.3100	0.2600	0.2100	0.1600	0.0010

Table 8. Parametric variation of *c*/D (B4-80 propeller)

B4-80	**r/R**	**0.2**	**0.3**	**0.4**	**0.5**	**0.6**	**0.7**	**0.8**	**0.9**	**1.0**
	Original	0.3324	0.3764	0.4100	0.4304	0.4374	0.4288	0.3940	0.3164	0.0010
Group 1. c/D constant along the blade	Alteration 1	0.2000	0.2000	0.2000	0.2000	0.2000	0.2000	0.2000	0.1800	0.0010
	Alteration 2	0.2200	0.2200	0.2200	0.2200	0.2200	0.2200	0.2200	0.2000	0.0010
	Alteration 3	0.2500	0.2500	0.2500	0.2500	0.2500	0.2500	0.2500	0.2200	0.0010
	Alteration 4	0.2800	0.2800	0.2800	0.2800	0.2800	0.2800	0.2800	0.2500	0.0010
	Alteration 5	0.3100	0.3100	0.3100	0.3100	0.3100	0.3100	0.3100	0.2800	0.0010
	Alteration 6	0.3300	0.3300	0.3300	0.3300	0.3300	0.3300	0.3300	0.3000	0.0010
	Alteration 7	0.3700	0.3700	0.3700	0.3700	0.3700	0.3700	0.3700	0.3450	0.0010
	Alteration 8	0.3900	0.3900	0.3900	0.3900	0.3900	0.3900	0.3900	0.3700	0.0010
	Alteration 9	0.4100	0.4100	0.4100	0.4100	0.4100	0.4100	0.4100	0.3900	0.0010
	Alteration 10	0.4250	0.4250	0.4250	0.4250	0.4250	0.4250	0.4250	0.4000	0.0010
Group 2. c/D decreases close to tip	Alteration 1	0.2000	0.2000	0.2000	0.2000	0.1750	0.1400	0.1050	0.0600	0.0010
	Alteration 2	0.2200	0.2200	0.2200	0.2200	0.1900	0.1600	0.1300	0.1000	0.0010
	Alteration 3	0.2500	0.2500	0.2500	0.2500	0.2250	0.1950	0.1550	0.1000	0.0010
	Alteration 4	0.2800	0.2800	0.2800	0.2800	0.2400	0.2000	0.1600	0.1150	0.0010
	Alteration 5	0.3100	0.3100	0.3100	0.3100	0.2700	0.2300	0.1900	0.1450	0.0010
	Alteration 6	0.3300	0.3300	0.3300	0.3300	0.2900	0.2500	0.2100	0.1600	0.0010
	Alteration 7	0.3700	0.3700	0.3700	0.3700	0.3300	0.2800	0.2200	0.1500	0.0010
	Alteration 8	0.3900	0.3900	0.3900	0.3900	0.3500	0.3100	0.2700	0.2300	0.0010
	Alteration 9	0.4100	0.4100	0.4100	0.4100	0.3600	0.3100	0.2700	0.2100	0.0010
	Alteration 10	0.4250	0.4250	0.4250	0.4250	0.3600	0.3000	0.2400	0.1700	0.0010

Table 9. Parametric variation of *c*/D (B5-60 propeller)

B5-60	**r/R**	**0.2**	**0.3**	**0.4**	**0.5**	**0.6**	**0.7**	**0.8**	**0.9**	**1.0**
	Original	0.1994	0.2258	0.246	0.2582	0.2624	0.2573	0.2364	0.1898	0.0010
Group 1. c/D constant along the blade	Alteration 1	0.1600	0.1600	0.1600	0.1600	0.1600	0.1600	0.1600	0.1000	0.0010
	Alteration 2	0.1800	0.1800	0.1800	0.1800	0.1800	0.1800	0.1800	0.1500	0.0010
	Alteration 3	0.1994	0.1994	0.1994	0.1994	0.1994	0.1994	0.1994	0.1500	0.0010
	Alteration 4	0.2258	0.2258	0.2258	0.2258	0.2258	0.2258	0.2258	0.1600	0.0010
	Alteration 5	0.2460	0.2460	0.2460	0.2460	0.2460	0.2460	0.2460	0.1800	0.0010
	Alteration 6	0.2582	0.2582	0.2582	0.2582	0.2582	0.2582	0.2582	0.2100	0.0010
	Alteration 7	0.2624	0.2624	0.2624	0.2624	0.2624	0.2624	0.2624	0.2100	0.0010
	Alteration 8	0.2900	0.2900	0.2900	0.2900	0.2900	0.2900	0.2900	0.2500	0.0010
	Alteration 9	0.3300	0.3300	0.3300	0.3300	0.3300	0.3300	0.3300	0.2700	0.0010
	Alteration 10	0.3500	0.3500	0.3500	0.3500	0.3500	0.3500	0.3500	0.2000	0.0010
Group 2. c/D decreases close to tip	Alteration 1	0.1650	0.1650	0.1650	0.1500	0.1400	0.1250	0.1100	0.0900	0.0010
	Alteration 2	0.1994	0.1994	0.1994	0.1994	0.1800	0.1600	0.1400	0.1150	0.0010
	Alteration 3	0.2258	0.2258	0.2300	0.2258	0.2000	0.1800	0.1600	0.1350	0.0010
	Alteration 4	0.2360	0.2360	0.2360	0.2150	0.1950	0.1700	0.1500	0.1350	0.0010
	Alteration 5	0.2460	0.2460	0.2460	0.2200	0.1900	0.1700	0.1500	0.1300	0.0010
	Alteration 6	0.2582	0.2582	0.2582	0.2300	0.2000	0.1700	0.1400	0.1100	0.0010
	Alteration 7	0.2700	0.2700	0.2700	0.2400	0.2100	0.1800	0.1500	0.1200	0.0010
	Alteration 8	0.2800	0.2800	0.2800	0.2600	0.2350	0.2150	0.1850	0.1500	0.0010
	Alteration 9	0.2900	0.2900	0.2900	0.2750	0.2550	0.2400	0.2250	0.2050	0.0010
	Alteration 10	0.3200	0.3200	0.3200	0.2900	0.2700	0.2450	0.2250	0.1900	0.0010

When consulting the tables above, it is possible see that, although the first group has constants *c*/D values, there is always a variation between the 0.8R and 0.9R positions. It happens because the geometries were adjusted to have a smoother form close to blade tip. This condition is necessary to avoid numerical problems of the algorithm.

Each parametric variation was analyzed with J ranging from 0.1 to 1.4. The results for the B3-45 propeller are shown in Figure 7, while the results for the B4-80 propeller are shown in Figure 8. Finally, the results for the B5-60 propeller can be seen in Figure 9. It is important to highlight that the OpenProp define the J range for the analyses, so the number and positions of the points aren't always the same.

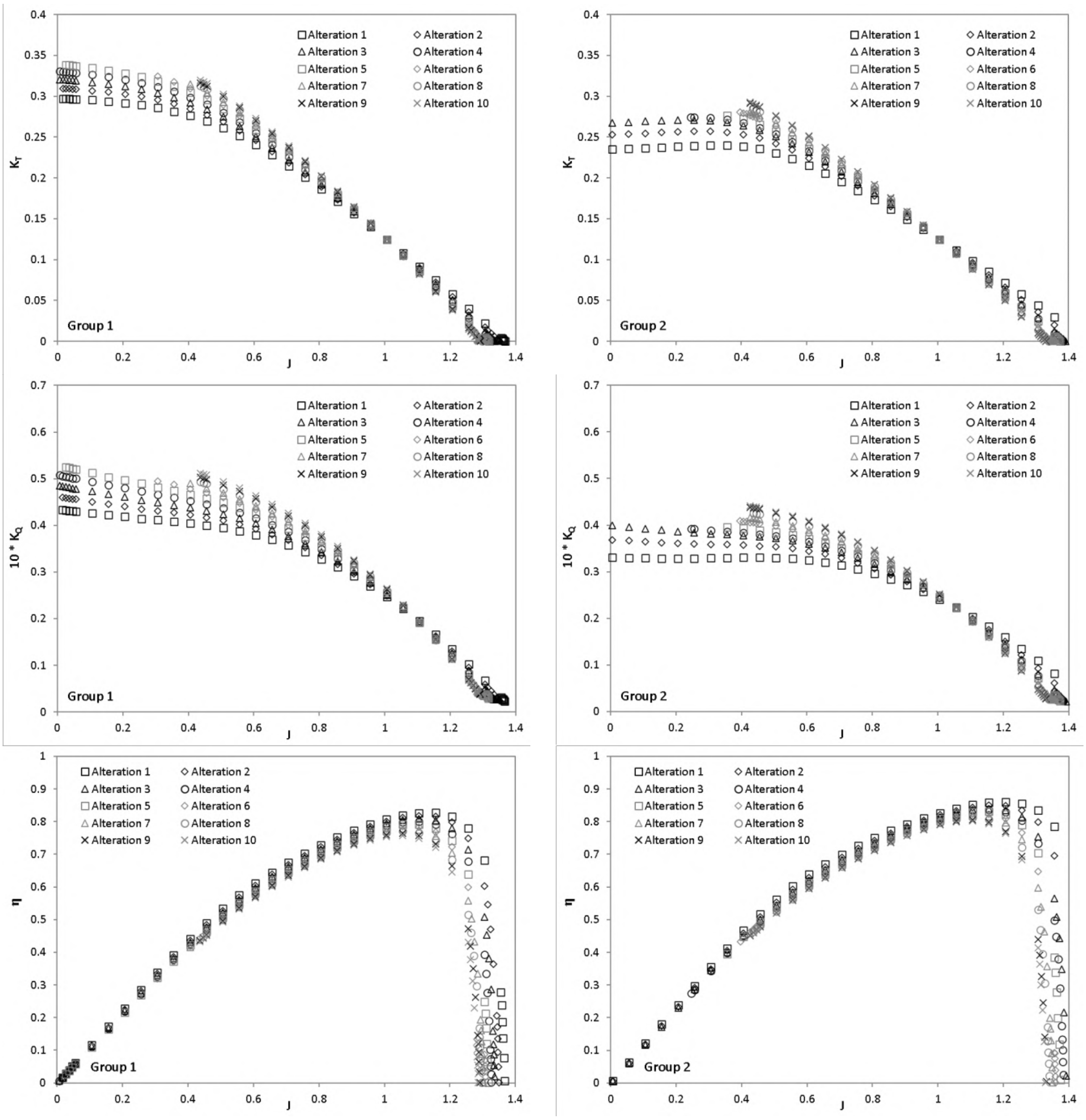

Figure 7. Performance results for the parametric variations of B3-45 propeller

The K_T results for the group 1 of parametric variations show that, to J lower than 0.8, the thrust decreases when lower c/D values are used. But, for J higher than 1.1, the thrust increases when lower c/D values are used. The same comportment is seen in K_Q results, but the variations are higher than seen in K_T results.

Finally, once the torque reductions are larger than thrust reductions, the efficient increases when lower c/D values are used. But in this case, the efficiency gain is highest when J is between 0.8 and 1.3. After this point, the propeller is very close to zero thrust condition and the results are not reliable or even useful.

Analyzing the graphs of the parameters K_T, K_Q and η for the parametric variations of group 2, similar results were observed, but with even more pronounced increases and decreases trends.

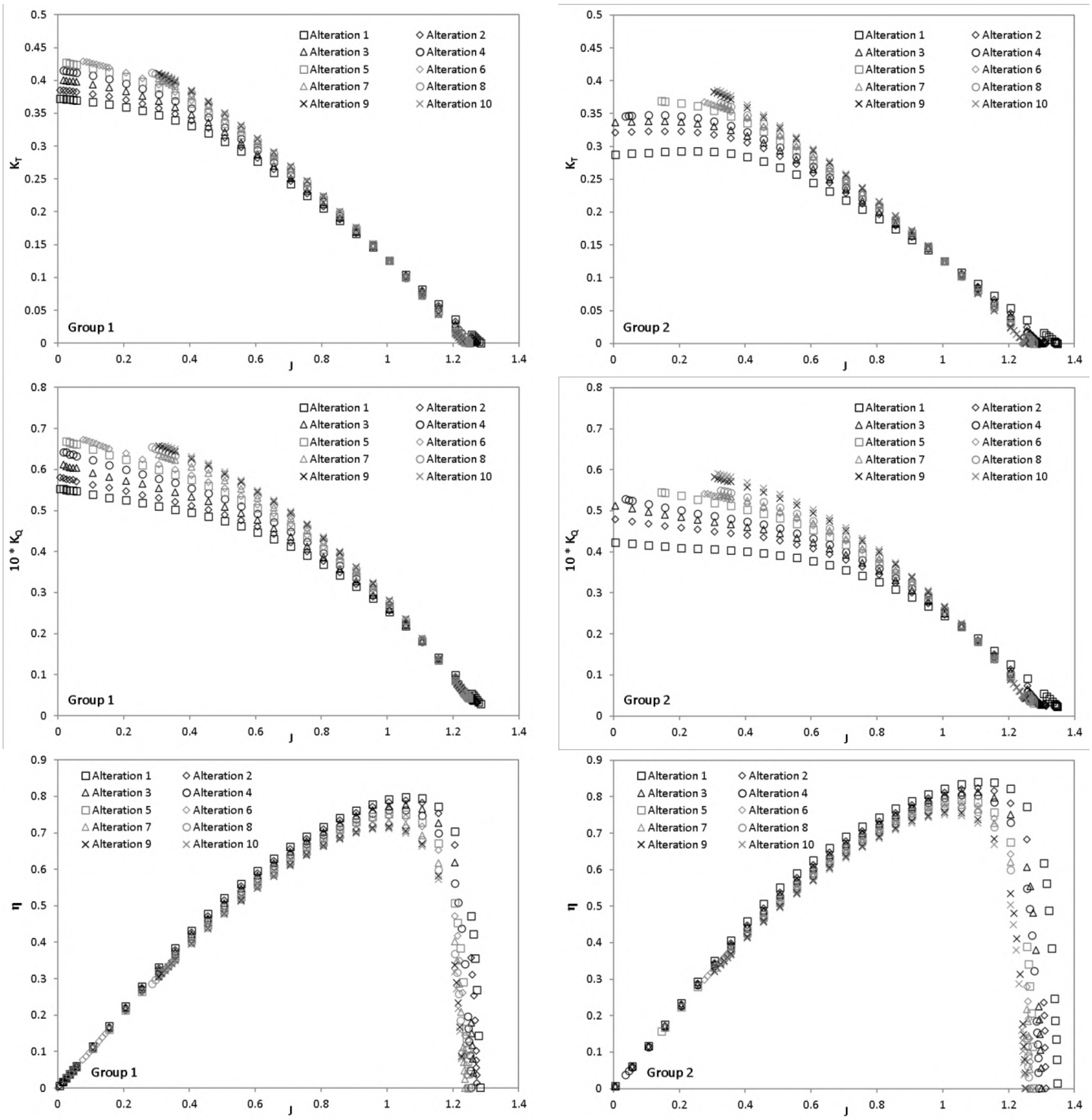

Figure 8. Performance results for the parametric variations of B4-80 propeller

Finally, the results for the B4-80 propeller (Figure 8) and B5-60 propeller (Figure 9) showed strictly the same behavior observed in the analysis of the B3-45 propeller (Figure 7).

To quantify the influence of *c*/D distribution, the results of all 189 variations were compared considering the same thrust requirement. The use of the same thrust requirement allows to compare the same operation point for different geometries. The results for each one of geometry are shown in Tables 10 to 12.

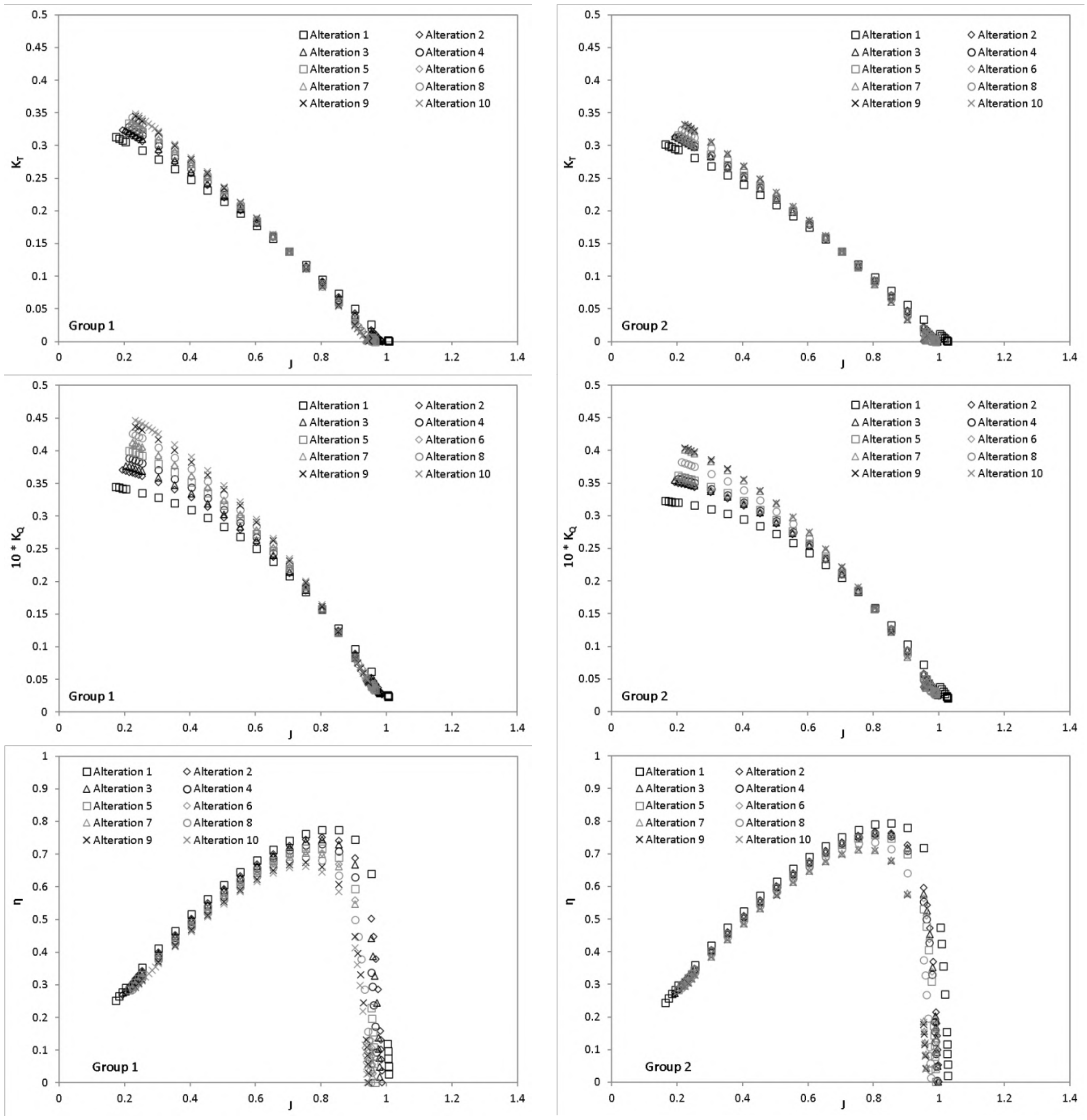

Figure 9. Performance results for the parametric variations of B5-60 propeller

The results of Table 10 to 12 shown that, considering the same operation point, the propellers performance respect the trends described before. In this case, the best results were reached by propeller B4-80. The efficiency of alteration 1 of group 1 increased 9.1% in relation to the original geometry B4-80, while the alteration 1 of group 2 increased 13.4%. Both variations had the lower values of *c*/D along the blade.

In the other hand, the worst performances were reached by propeller B5-45. The efficiency of alteration 10 of group 1 decreased 7.0% in relation to the original geometry B5-45, while the efficiency of alteration 10 of group 2 decreased 2.2%. Both variations had the higher *c*/D values along the blades.

Table 10. Results for advance coefficient *J* equal 1 to the B3-45, B3-60 e B3-80 propellers

B3 propeller variations		**EAR = 0.45**					**EAR = 0.60**					**EAR = 0.80**				
		K_T	**$10*K_Q$**	**η**	**EAR**	**P/D**	**K_T**	**$10*K_Q$**	**η**	**EAR**	**P/D**	**K_T**	**$10*K_Q$**	**η**	**EAR**	**P/D**
	Original	0.125	0.258	0.773	0.450	1.178	0.118	0.253	0.747	0.599	1.167	0.161	0.360	0.716	0.799	1.230
Group 1. c/D constant along the blade	Alteration 1	0.125	0.247	0.807	0.269	1.181	0.118	0.239	0.789	0.375	1.169	0.161	0.331	0.778	0.329	1.235
	Alteration 2	0.125	0.249	0.801	0.300	1.180	0.118	0.241	0.782	0.406	1.168	0.161	0.333	0.774	0.359	1.233
	Alteration 3	0.125	0.251	0.795	0.331	1.178	0.118	0.243	0.776	0.437	1.167	0.161	0.335	0.769	0.390	1.231
	Alteration 4	0.125	0.253	0.789	0.362	1.177	0.118	0.245	0.770	0.468	1.167	0.161	0.337	0.765	0.421	1.230
	Alteration 5	0.125	0.255	0.783	0.393	1.176	0.118	0.247	0.763	0.498	1.166	0.161	0.339	0.760	0.452	1.229
	Alteration 6	0.125	0.257	0.777	0.424	1.176	0.118	0.249	0.758	0.529	1.166	0.161	0.341	0.756	0.483	1.228
	Alteration 7	0.125	0.259	0.771	0.455	1.175	0.118	0.251	0.753	0.561	1.166	0.161	0.343	0.752	0.514	1.227
	Alteration 8	0.125	0.261	0.765	0.486	1.175	0.118	0.253	0.747	0.592	1.165	0.161	0.345	0.747	0.545	1.227
	Alteration 9	0.125	0.263	0.760	0.517	1.175	0.118	0.256	0.741	0.629	1.165	0.161	0.346	0.743	0.576	1.226
	Alteration 10	0.125	0.264	0.754	0.548	1.175	0.118	0.257	0.736	0.654	1.165	0.161	0.348	0.739	0.607	1.226
Group 2. c/D decreases close to tip	Alteration 1	0.125	0.241	0.827	0.214	1.213	0.118	0.231	0.816	0.302	1.191	0.161	0.324	0.796	0.263	1.230
	Alteration 2	0.125	0.243	0.820	0.245	1.200	0.118	0.232	0.812	0.325	1.187	0.161	0.325	0.791	0.294	1.270
	Alteration 3	0.125	0.245	0.815	0.274	1.195	0.118	0.234	0.808	0.350	1.184	0.161	0.327	0.788	0.316	1.257
	Alteration 4	0.125	0.245	0.812	0.295	1.195	0.118	0.235	0.802	0.382	1.181	0.161	0.327	0.787	0.337	1.253
	Alteration 5	0.125	0.246	0.809	0.316	1.194	0.118	0.236	0.799	0.405	1.179	0.161	0.329	0.783	0.365	1.249
	Alteration 6	0.125	0.248	0.804	0.345	1.192	0.118	0.238	0.794	0.429	1.178	0.161	0.331	0.779	0.395	1.247
	Alteration 7	0.125	0.249	0.801	0.370	1.190	0.118	0.239	0.790	0.456	1.176	0.161	0.332	0.776	0.420	1.244
	Alteration 8	0.125	0.250	0.796	0.396	1.188	0.118	0.240	0.786	0.478	1.175	0.161	0.334	0.772	0.451	1.240
	Alteration 9	0.125	0.252	0.791	0.424	1.186	0.118	0.242	0.780	0.511	1.173	0.161	0.336	0.767	0.480	1.236
	Alteration 10	0.125	0.253	0.790	0.443	1.186	0.118	0.245	0.770	0.550	1.171	0.161	0.338	0.763	0.511	1.234

Table 11. Results for advance coefficient *J* equal 1 to the B4-45, B4-60 e B4-80 propellers

B4 propeller variations		**EAR = 0.45**					**EAR = 0.60**					**EAR = 0.80**				
		K_T	**$10*K_Q$**	**η**	**EAR**	**P/D**	**K_T**	**$10*K_Q$**	**η**	**EAR**	**P/D**	**K_T**	**$10*K_Q$**	**η**	**EAR**	**P/D**
	Original	0.142	0.291	0.782	0.449	1.186	0.135	0.284	0.759	0.599	1.173	0.125	0.276	0.726	0.799	1.160
Group 1. c/D constant along the blade	Alteration 1	0.142	0.284	0.802	0.322	1.187	0.135	0.274	0.786	0.424	1.174	0.125	0.253	0.792	0.404	1.162
	Alteration 2	0.142	0.285	0.797	0.356	1.187	0.135	0.276	0.781	0.462	1.174	0.125	0.256	0.784	0.445	1.162
	Alteration 3	0.142	0.286	0.794	0.371	1.186	0.135	0.278	0.775	0.495	1.173	0.125	0.259	0.774	0.503	1.160
	Alteration 4	0.142	0.290	0.784	0.426	1.183	0.135	0.281	0.768	0.536	1.172	0.125	0.263	0.763	0.565	1.159
	Alteration 5	0.142	0.292	0.778	0.467	1.182	0.135	0.283	0.762	0.569	1.172	0.125	0.267	0.752	0.627	1.159
	Alteration 6	0.142	0.294	0.773	0.496	1.182	0.135	0.285	0.756	0.600	1.172	0.125	0.269	0.745	0.668	1.159
	Alteration 7	0.142	0.296	0.769	0.524	1.182	0.135	0.288	0.750	0.641	1.171	0.125	0.275	0.730	0.753	1.159
	Alteration 8	0.142	0.299	0.760	0.577	1.181	0.135	0.289	0.746	0.667	1.171	0.125	0.278	0.723	0.797	1.159
	Alteration 9	0.142	0.301	0.755	0.608	1.180	0.135	0.290	0.743	0.689	1.171	0.125	0.280	0.716	0.839	1.159
	Alteration 10	0.142	0.303	0.750	0.646	1.180	0.135	0.293	0.737	0.729	1.171	0.125	0.282	0.712	0.868	1.159
Group 2. c/D decreases close to tip	Alteration 1	0.142	0.279	0.816	0.277	1.200	0.135	0.266	0.812	0.347	1.188	0.125	0.244	0.823	0.320	1.189
	Alteration 2	0.142	0.280	0.811	0.308	1.197	0.135	0.268	0.804	0.388	1.183	0.125	0.247	0.811	0.368	1.173
	Alteration 3	0.142	0.281	0.809	0.322	1.195	0.135	0.270	0.799	0.416	1.182	0.125	0.250	0.803	0.421	1.174
	Alteration 4	0.142	0.284	0.801	0.371	1.191	0.135	0.272	0.793	0.458	1.180	0.125	0.252	0.798	0.461	1.170
	Alteration 5	0.142	0.286	0.795	0.409	1.190	0.135	0.272	0.792	0.474	1.181	0.125	0.255	0.786	0.523	1.167
	Alteration 6	0.142	0.287	0.792	0.431	1.188	0.135	0.274	0.787	0.501	1.179	0.125	0.258	0.779	0.526	1.166
	Alteration 7	0.142	0.288	0.782	0.457	1.189	0.135	0.274	0.787	0.520	1.181	0.125	0.259	0.774	0.618	1.167
	Alteration 8	0.142	0.291	0.782	0.503	1.187	0.135	0.275	0.783	0.544	1.180	0.125	0.261	0.770	0.644	1.165
	Alteration 9	0.142	0.291	0.780	0.523	1.187	0.135	0.278	0.775	0.583	1.177	0.125	0.267	0.751	0.704	1.163
	Alteration 10	0.142	0.293	0.775	0.561	1.186	0.135	0.279	0.772	0.610	1.177	0.125	0.263	0.751	0.739	1.162

Table 12. Results for advance coefficient *J* equal 0.7 to the B5-45, B5-60 e B5-80 propellers

B5 propeller variations		**EAR = 0.45**					**EAR = 0.60**					**EAR = 0.80**				
		K_T	**$10*K_Q$**	**η**	**EAR**	**P/D**	**K_T**	**$10*K_Q$**	**η**	**EAR**	**P/D**	**K_T**	**$10*K_Q$**	**η**	**EAR**	**P/D**
	Original	0.142	0.220	0.724	0.449	0.889	0.138	0.220	0.701	0.599	0.880	0.132	0.220	0.670	0.799	0.872
Group 1. c/D constant along the blade	Alteration 1	0.142	0.213	0.750	0.299	0.895	0.138	0.209	0.741	0.385	0.889	0.132	0.204	0.722	0.477	0.874
	Alteration 2	0.142	0.216	0.739	0.361	0.891	0.138	0.213	0.726	0.449	0.883	0.132	0.208	0.708	0.554	0.872
	Alteration 3	0.142	0.218	0.731	0.411	0.891	0.138	0.214	0.721	0.491	0.885	0.132	0.213	0.693	0.634	0.871
	Alteration 4	0.142	0.220	0.724	0.449	0.888	0.138	0.217	0.712	0.552	0.884	0.132	0.215	0.688	0.670	0.871
	Alteration 5	0.142	0.224	0.714	0.505	0.886	0.138	0.220	0.703	0.603	0.882	0.132	0.219	0.673	0.760	0.870
	Alteration 6	0.142	0.226	0.705	0.556	0.885	0.138	0.222	0.695	0.642	0.880	0.132	0.222	0.664	0.827	0.870
	Alteration 7	0.142	0.229	0.698	0.614	0.884	0.138	0.223	0.692	0.655	0.880	0.132	0.224	0.658	0.861	0.870
	Alteration 8	0.142	0.232	0.689	0.659	0.884	0.138	0.227	0.680	0.728	0.878	0.132	0.229	0.644	0.952	0.870
	Alteration 9	0.142	0.235	0.679	0.724	0.883	0.138	0.231	0.668	0.821	0.878	0.132	0.231	0.638	0.991	0.870
	Alteration 10	0.142	0.237	0.673	0.763	0.883	0.138	0.235	0.659	0.878	0.878	0.132	0.233	0.632	1.038	0.870
Group 2. c/D decreases close to tip	Alteration 1	0.142	0.209	0.765	0.258	0.910	0.138	0.206	0.751	0.350	0.891	0.132	0.197	0.749	0.400	0.884
	Alteration 2	0.142	0.210	0.759	0.302	0.908	0.138	0.210	0.736	0.440	0.889	0.132	0.198	0.745	0.453	0.887
	Alteration 3	0.142	0.213	0.751	0.351	0.900	0.138	0.210	0.734	0.469	0.887	0.132	0.203	0.726	0.540	0.879
	Alteration 4	0.142	0.215	0.744	0.390	0.897	0.138	0.211	0.732	0.490	0.887	0.132	0.204	0.725	0.560	0.880
	Alteration 5	0.142	0.217	0.734	0.441	0.892	0.138	0.212	0.729	0.504	0.885	0.132	0.207	0.714	0.636	0.877
	Alteration 6	0.142	0.219	0.730	0.477	0.892	0.138	0.211	0.732	0.511	0.888	0.132	0.209	0.706	0.691	0.876
	Alteration 7	0.142	0.222	0.721	0.538	0.889	0.138	0.221	0.701	0.664	0.883	0.132	0.209	0.706	0.708	0.877
	Alteration 8	0.142	0.222	0.719	0.562	0.891	0.138	0.217	0.715	0.595	0.884	0.132	0.211	0.701	0.768	0.877
	Alteration 9	0.142	0.224	0.714	0.608	0.891	0.138	0.221	0.698	0.658	0.879	0.132	0.213	0.693	0.797	0.875
	Alteration 10	0.142	0.225	0.708	0.646	0.890	0.138	0.221	0.699	0.690	0.881	0.132	0.215	0.685	0.859	0.874

6. CONCLUSIONS

This work presented an extensive parametric analysis of the influence of c/D quotient distribution on the hydrodynamic performance of Wageningen B-Series propellers. The Lifting-line Theory was used, whose limitations include, for example, the negligence of the compressibility and viscosity of the fluid.

Regarding the validation of the technique/tool, it was observed a difficult to obtain a geometric model that reproduces the propeller design characteristics. In many cases, the modeled propeller did not match with the design model. No specific reason was found. In this case, the only recommendation is an iterative modeling procedure, feeding back the input data until the modeled geometry match with design parameters.

In validation phase, the analyses of the B4-85 propeller shown that the performance curves obtained were close to experimental data provided by Kuiper (1992). The differences found can be attributed, in part, to the fact that the Lifting-line Theory analyzes the sections individually, disregarding the flow three-dimensional aspects and the interaction between adjacent blades.

The preliminary results were good enough to justify the application of this methodology in the preliminary analysis of propellers, especially in the cases where the is no experimental data.

The parametric phase analyzed 189 variations grouped in 9 propellers of Wageningen B-Series. The results shown that the distribution of *c*/D has low impact on the hydrodynamic performance when the advance coefficient J is between 0.8 and 1.1. However, the results shown greater differences when J is outside this range.

When lower *c*/D values than original geometry are used, the K_T and K_Q decreased when J is lower than 0.8 and they increased when J is higher than 1.1. So, in cases of low propeller rotation (J higher than 1.1) the thrust will increase with lower c/D values. But, in the cases of high propeller rotation (J lower than 0.8) the thrust will decrease.

The analyses showed an opposite behavior for the efficiency, with significant differences when the advance coefficient J is between 0.8 and 1.2. In this case, the efficiency increases with lower *c*/D values than original geometry.

The results were consistent and allow us to inference that the smaller the value of *c*/D, the greater the efficiency of a propeller. Finally, when lower *c*/D values are used close to the blade's tips, the efficiency increments are even greater. In the cases analyzed, the higher efficiency increment using constant *c*/D values along the blade was 9%. Nonetheless, when was used variations with lower *c*/D close to blade's tips, the efficiency increment reached 13%.

Although these results accord with Kuiper (1992), it is necessary to highlight that, as seen in Gerr (1989), the propellers hydrodynamic performance are limited by structural and cavitation aspects. In this case, it is well documented that the *c*/D reduction can provoke cavitation on the blades. So, it is a multi-objective interesting problem of design to try maximizing the hydrodynamic efficiency and minimize the cavitation levels of a propeller.

7. REFERENCES

Abbott, I. H., Doenhoff, A. E. V., 1959. “Theory of Wing Sections: Including a Summary of Airfoil Data”. Dover Publications, New York.

Anderson, J. D., 2001. “Fundamentals of Aerodynamics”. McGraw Hill Inc., New York.

Carlton, J., 2007. “Marine Propellers and Propulsion”. Butterworth-Heinemann, United Kingdom.

Dartmouth College. *OpenProp: Integrated rotor design and analysis*, Engineering Dartmouth, https://engineering.dartmouth.edu/openprop/. Accessed in 28 April 2019.

Epps, B. P., 2016. “On the rotor lifting line wake model”. *Journal of Ship Production and Design*, Vol. 32, No. 3, pp. 31-45.

Epps, B. P., Kimball, R. W., 2013. “Unified Rotor Lifting Line Theory”. *Journal of Ship Research*, Vol. 57, No. 4, pp. 181-201.

Gerr, D., 1989. “Propeller Handbook: The Complete Reference for Choosing, Installing and Understanding Boat Propellers”. International Marine Pub Co, United States of America.

Kuiper, G., 1992. “The Wageningen Propeller Series”. Marin Publication, Wageningen.

Lammeren, W., 1936. Resultaten van Systematische Proeven met Vrij-varende 4-bladige Schroeven, type A4.40. N.S.M.B, Wageningem, p. 140-144.

Lammeren, W.; Oosterveld, M., 1969. The Wageningen B-screw Series. Wageningen, The Netherlands: Netherlands Ship Model Basin.

Lammeren, W.; Troost, L., 1948. Resistance, Propulsion and Steering of Ships: A Manual for Designing Hull Forms, Propellers and Rudders. 2. ed. Wageningem, The Netherlands: Ships and Marine Engines.

MacPherson, D. 2020. “Modelling contemporary propellers with traditional series”. Riviera Maritime Media Ltd. https://www.rivieramm.com/news-content-hub/news-content-hub/modelling-contemporary-propellers-with-traditional-series-61169. Accessed in 02/09/2021.

Mises, R., 1959. “Theory of Flight”. Dover Publications, New York.

Molland, A. F., 2008. “The Maritime Engineering Reference Book: A Guide to Ship Design, Construction and Operation”. Elsevier Science Ltd., Oxford.

Watson, D. G. M., 1998. “Practical Ship Design”. Elsevier Science Ltd, Oxford.

8. RESPONSIBILITY NOTICE

The authors are the only responsible for the printed material included in this paper.

9. ANNEX 1 - WAGENINGEN B4-80 PROPELLER VARIATIONS

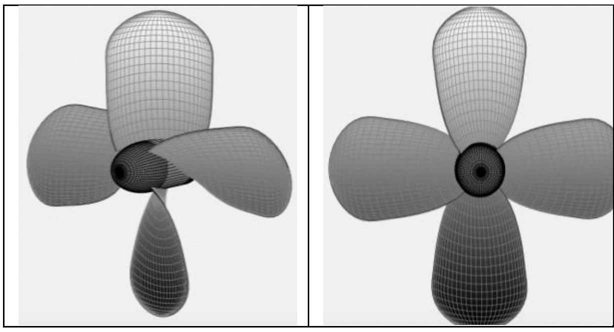
Propeller G1-A1

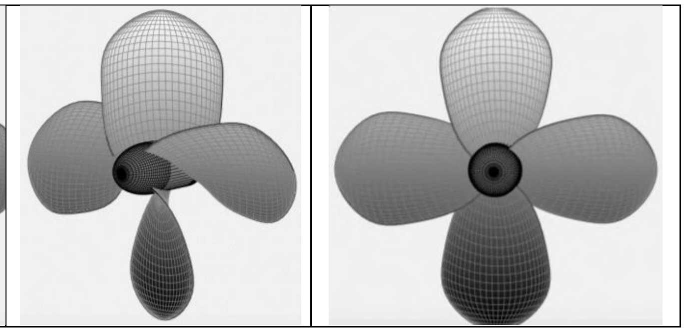
Propeller G2-A2

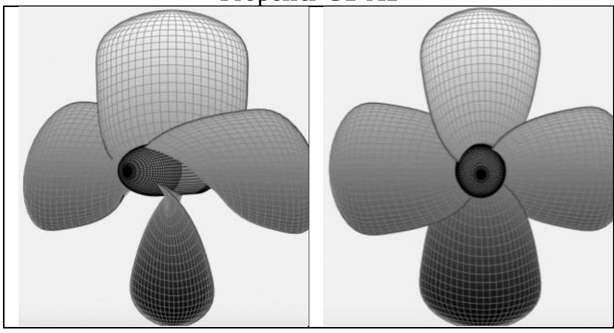
Propeller G1-A3

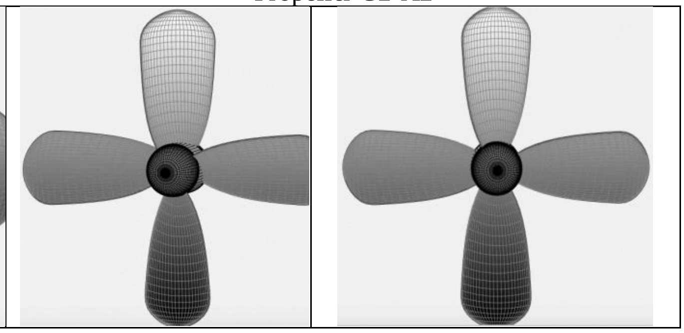
Propeller G1-A4

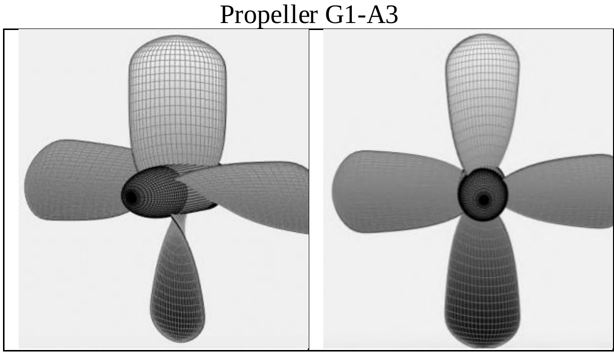
Propeller G1-A5

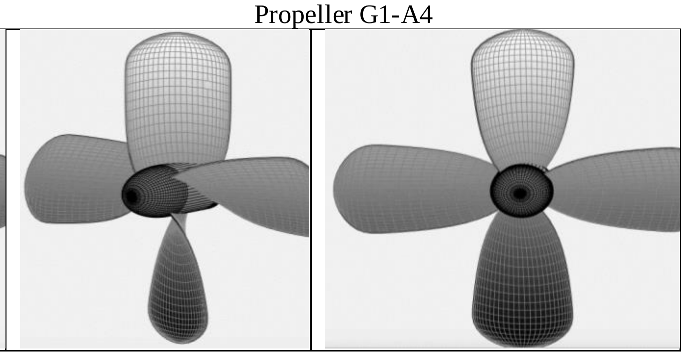
Propeller G1-A6

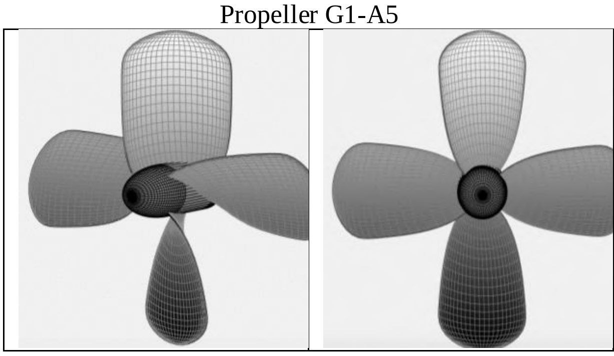
Propeller G1-A7

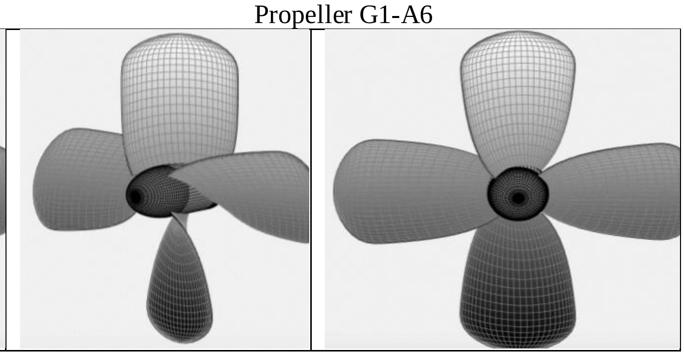
Propeller G1-A8

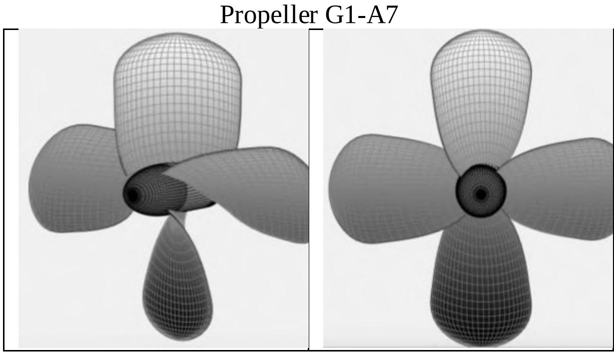
Propeller G1-A9

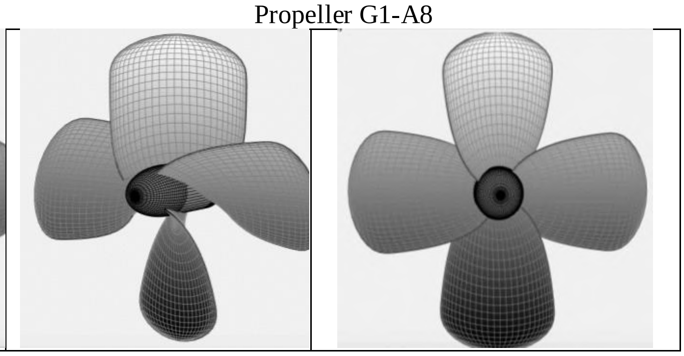
Propeller G1-A10

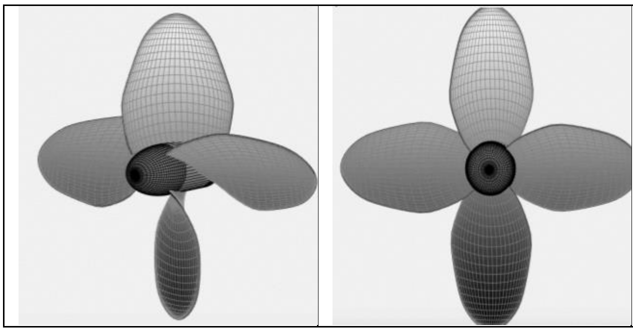

Propeller G2-A1

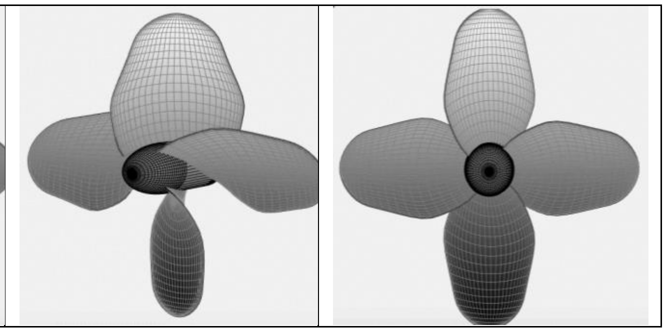

Propeller G2-A2

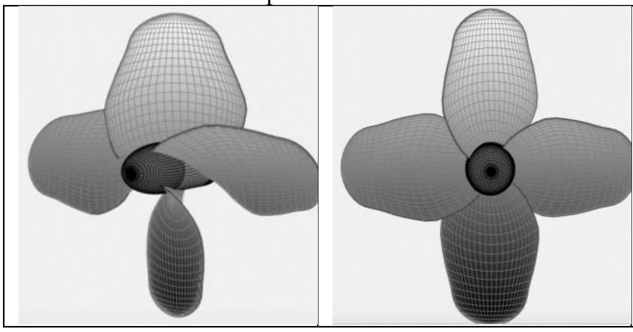

Propeller G2-A3

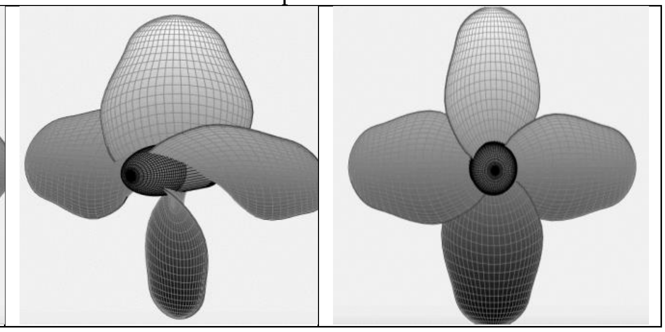

Propeller G2-A4

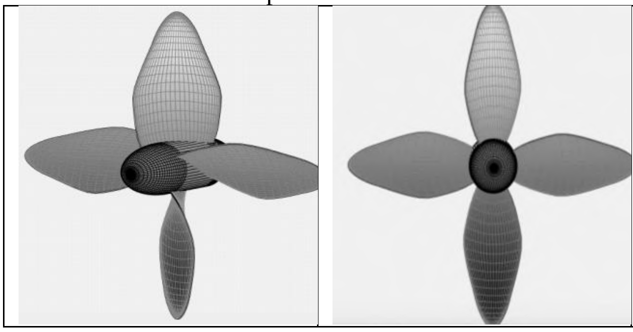

Propeller G2-A5

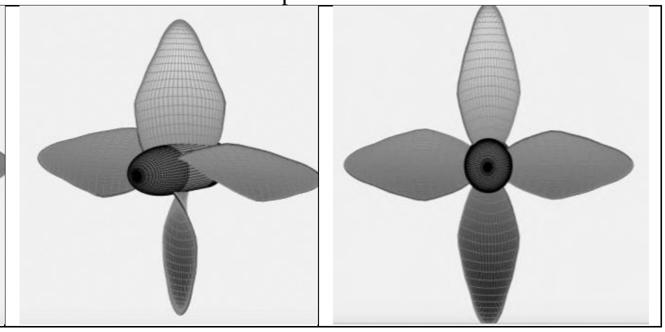

Propeller G2-A6

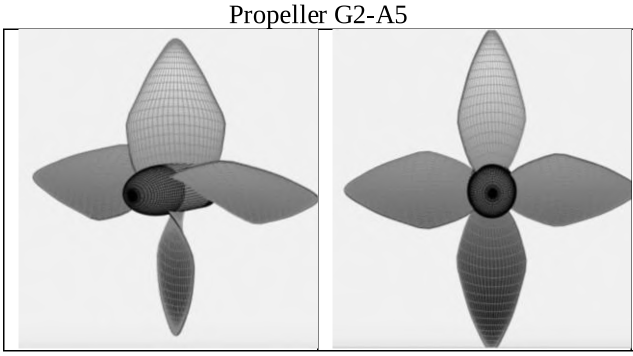

Propeller G2-A7

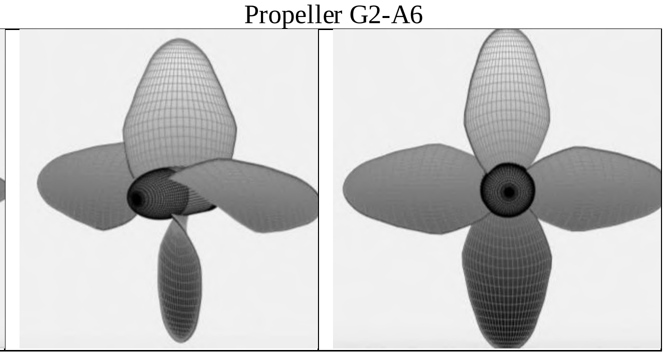

Propeller G2-A8

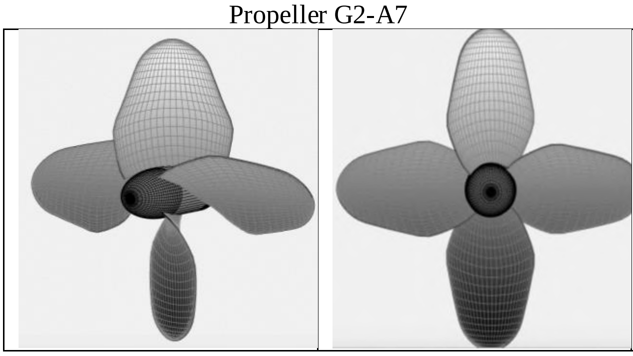

Propeller G2-A9

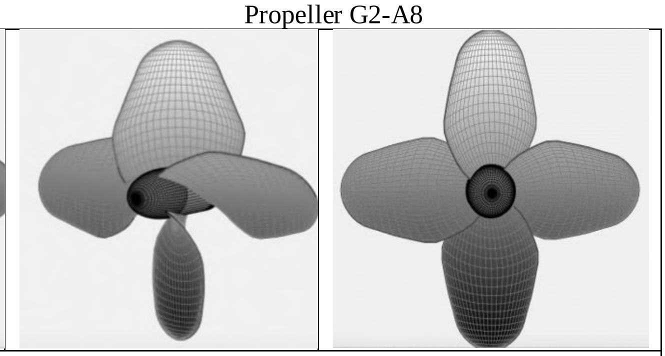

Propeller G2-A10